International Journal of Applied Mathematics

Volume 38 No. 12s, 2025

ISSN: 1311-1728 (printed version); ISSN: 1314-8060 (on-line version)

SHIP DETECTION AND CLASSIFICATION USING YOLOV8 THROUGH TRANSFER LEARNING APPROACH

Kolli Sujit[*1], Kesavadev Varikattu Karottu[2], Siva Prasad Kodungallur[3], Sheeja Janardhan[4]

[1,2,4] Department of Naval Architecture and Ocean Engineering, Indian Maritime University, Visakhapatnam-530035, India.

Kolli.sujit@gmail.com, vkkesavadev@imu.ac.in, sheejaaj@imu.ac.in

[3]Department of Ship Technology, Cochin University of Science and Technology. Kochi, India.

sivachinta1965@gmail.com

Abstract

In urgent situations such as maritime disasters rapid vessel detection and tracking are vital for coordinating search and rescue, as well as for enabling autonomous navigation and collision avoidance systems. This study evaluates the use of YOLOv8m, a high-performance one-stage deep-learning detector, to locate ships in profile imagery and categorize them by type. By adopting a transfer-learning strategy, we fine-tune a pre-trained YOLOv8m model on a diverse compilation of open-source ship photographs, adapting its general object-recognition capabilities to this specialized maritime task. We report on the model's performance measured by detection recall, precision, and classification accuracy demonstrating its suitability for real-time ship identification in varied operational scenarios. And testing with various classes for ship identification.

Math Subject Classification 2020: 68T07, 68T45

Keywords: Ship detection, Ship classification, YOLOv8m, Transfer learning, Maritime surveillance

1.Introduction

Deep-learning based ship localization and tracking systems increasingly rely on one-stage architectures for end-to-end speed and simplicity (Jiang et al. [6]; Zheng & Zhang [38]). Among these, YOLOv8 has emerged as a leading framework for maritime surveillance owing to its real-time throughput and competitive accuracy on optical and SAR imagery (Matasci et al. [16]). Operational rescue and collision-avoidance applications demand both rapid inference and high detection fidelity. Improved YOLO variants such as the YOLOv4-and YOLOv5-based methods demonstrate microsecond-scale processing while maintaining over 85 % mean average precision on vessel datasets (He et al. [3]; Kim et al. [9]; Jiang et al. [5]). Maritime scenes present challenges like fog, glare, low light, and changing sea states. Multi-resolution SAR ship datasets and synthetic-target IR benchmarks help models generalize beyond clear-day, calm-sea conditions (Humayun et al. [4]; Jiang et al. [5]). Incorporating both

Volume 38 No. 12s, 2025

ISSN: 1311-1728 (printed version); ISSN: 1314-8060 (on-line version)

optical and radar modalities further bolsters performance under adverse weather and illumination shifts Liu et al. [12]; Li & Man, [10]. The maritime domain includes fishing boats, container ships, tankers, and more all with distinct silhouettes. To discriminate among these classes, deep networks must train on richly annotated, multi-class ship collections Cheng et al. [1]; Song et al. [21]. Recent multi-scale detection approaches achieve over 90 % classification accuracy across more than five vessel categories Yasir et al. [34]; Kim et al. [9]. Fine-tuning pre-trained YOLOv8 backbones on aggregated ship imagery spanning UAV, satellite, and drone sources enables rapid adaptation to maritime contexts with limited labelled data Li et al. [11]. This transfer-learning paradigm significantly reduces training time while preserving strong generalization across unseen environments Cheng et al. [1]

Accurate vessel monitoring hinges on minimizing both false alarms and missed detections, as misidentification can jeopardize maritime safety and security. Regulatory frameworks such as the IMO's Port State Control inspections further drive the development of reliable detection systems. Yet, despite numerous publicly available ship datasets (from drone, optical, infrared, and SAR sources), limited sample sizes and uneven coverage of extreme weather or specific regions can hinder model generalization. Ultralytics' YOLOv8 sets new standards in speed and precision compared to earlier YOLO iterations, and integrating advanced modules like generative data augmentation and the LW-Swin transformer with residual, scaled-normalization blocks can further boost robustness and accuracy.

Reducing false positives and negatives is critical, since classification errors in ship detection systems pose serious threats to maritime security and operational safety Cong-An et al., [2]. Adhering to established maritime regulations such as the IMO's Port State Control, which verifies vessel and equipment compliance with international safety instruments serves as a catalyst for advancing detection and tracking models' reliability (IMO, 2025) Ongoing enhancements in deep-learning architectures facilitate seamless integration with broader maritime surveillance technologies, ensuring consistent performance under operational constraints Matasci et al. [16]

Model development and evaluation have leveraged a variety of ship imagery collections, including drone-captured optical images Cheng et al. [1] and SAR datasets employing feature-aligned detectors Cong-An et al. [2]. Nevertheless, many publicly shared datasets remain relatively small, which can restrict a network's ability to generalize across unseen environments and rare conditions Yasir et al. [34]. In regions or weather regimes lacking sufficient annotated examples such as storms or ice-covered waters performance may degrade significantly Lou et al. [13].

The YOLO family has revolutionized real-time object detection, and YOLOv8 now leads with an anchor-free head, optimized backbone/neck, and enhanced speed–accuracy trade-offs over YOLOv5 and YOLOv7. Beyond raw architecture, data augmentation via generative models expands input diversity, while the LW-Swin transformer module augmented with a residual network incorporating scaled normalization and learnable parameters improves long-range context modelling and feature fusion for small and distant targets

Volume 38 No. 12s, 2025

ISSN: 1311-1728 (printed version); ISSN: 1314-8060 (on-line version)

2.Literature Survey

2.1 Conventional methods

The object detection task at sea hinges on accurately defining the Region of Interest (ROI), with the horizon or sea sky line (SSL) being especially critical. Classical SSL-based ROI methods typically follow three core stages: image preprocessing Song et al., [21], feature extraction Wang et al. [26], and object classification Wu et al. [27]. These steps closely parallel those in terrestrial detection systems. Much of the literature has focused on precise SSL estimation techniques: Ma et al. [15] first fit candidate lines via a least-squares criterion and then applied non-linear suppression to select the optimal horizon; Xin et al. [29] utilized the Hough transform on pre-filtered imagery, iteratively tuning thresholds to refine the detected line's alignment. Other notable SSL determination approaches include the Radon transform Prasad et al. [19] and RANSAC-based line fitting Song et al. [22]; Wang et al. [25]

Dynamic ROI extraction zeroes in on moving maritime objects by distinguishing them from static backgrounds. Yang et al. [31] devised an adaptive inter-frame differencing algorithm that highlights slowly moving vessel segments through frame-to-frame subtraction, effectively suppressing ambient noise.

Background-subtraction methods offer an alternative: rather than direct frame differencing, they first construct a background model and then subtract it to isolate foreground ROIs. Xiao et al. [28] implemented a visual background extractor that continuously updates scene parameters, boosting detection accuracy for small or distant objects by incorporating richer background features. Optical-flow–based ROI delineation has also been explored Li & Man, [10]

While these traditional techniques benefit from low computational overhead, straightforward parameterization, and real-time performance, they often struggle with drastic changes in illumination, weather, and sea state and require manual adjustment limiting their robustness in complex maritime environments.

2.2 Deep learning methodologies

With the continuous enhancements in GPU and parallel computing technologies, deep learning has become the predominant approach for marine object detection since around 2012. Two pillars underpin the success of these methods: the availability of diverse, well-annotated datasets and the design of effective neural architectures. However, publicly available maritime datasets remain limited in scale and scope, including MCShips Zheng & Zhang. [38], the Singapore Maritime Dataset (SMD) Kim et al. [9], SeaSHIPS, and ABOShips among a few others. Since dataset characteristics heavily influence both accuracy and inference speed, models trained on one collection may exhibit degraded performance when deployed across different sea states, lighting conditions, or sensor modalities.

Convolutional neural networks (CNNs) are the de facto backbone for modern ship detectors, which split broadly into anchor-free and anchor-based categories. Anchor-free methods dispense with preset bounding boxes, offering simpler pipelines and reduced computational

Volume 38 No. 12s, 2025

ISSN: 1311-1728 (printed version); ISSN: 1314-8060 (on-line version)

overhead; prominent examples include FCOS Tian et al. [24] and RepPoints Yang et al. [33]. Despite their speed advantages, these approaches often fall slightly behind in raw detection precision compared to anchor-based frameworks. Anchor-based detectors, by contrast, rely on predefined box priors to propose candidates. One-stage models like SSD and YOLO fuse localization and classification in a single pass, whereas two-stage architectures (e.g., Faster R-CNN Qi et al. [20], Mask R-CNN Nie et al. [18] first generate region proposals and then refine them, generally achieving higher accuracy at the cost of additional inference time.

To mitigate the challenges of limited data and computational constraints, researchers have developed lightweight and hybrid networks. Jin & Liu [7] augmented SSD with feature fusion and squeeze-and-excitation modules to boost small-ship detection accuracy to 94.41% mAP on the SSDD benchmark. MC-YOLOv5s replaces YOLOv5's backbone with MobileNetV3-Small and introduces a ConvNeXt-inspired fusion block, reducing parameters by nearly 7 MB while increasing mAP by 3.4%.

Despite significant strides in accuracy and robustness, deep learning detectors often demand longer processing times than classical methods a critical consideration for real-time shipborne or unmanned surface vehicle systems. Ongoing research therefore focuses on reconciling high detection fidelity with low latency through architectural optimizations and novel attention mechanisms.

2.3 The YOLO algorithm

The YOLO series exemplifies a family of single-stage detectors engineered to strike a balance between high detection fidelity and real-time inference Jiang et al. [6]. Thanks to their lightweight pipelines, these networks have been widely deployed in scenarios demanding immediate insights ranging from autonomous aerial searches on UAV platforms Li et al. [11] to threat assessment aboard uncrewed surface combatants. Building on YOLOv4, He et al. [3] incorporated a k-means–driven clustering step to refine anchor assignments, which led to notable gains in berth-approaching vessel detection. Meanwhile, Yang et al. [32] enhanced YOLOv5n by embedding a ShuffleNetV2-based attention block and multi-scale feature fusion ("add fusion"), boosting its capacity to distinguish and localize small, fast-moving boats. More recently, Zhao et al. [37] tailored YOLOv7 for maritime search-and-rescue by introducing SimAM modules parameter-free attention layers that sharpen region proposals and appending a dedicated tiny-object detection head to recover sub-pixel targets. Despite these advances, onboard maritime deployments still contend with occlusion from wave crests, sun glint, and diminutive object signatures; concurrently, the drive toward cost-effective, power-efficient processors places a premium on further slimming network footprints without sacrificing accuracy.

At the core of every YOLO variant lie three interdependent components: the backbone, which hierarchically extracts visual features; the neck, which merges multi-scale representations; and the head, where classification and bounding-box regression occur. In earlier iterations (up to YOLOv3), the neck relied on a Feature Pyramid Network (FPN) to aggregate features across scales. YOLOv4 and v5 introduced the PAN-FPN (Path Aggregation Network atop FPN) to

International Journal of Applied Mathematics

Volume 38 No. 12s, 2025

ISSN: 1311-1728 (printed version); ISSN: 1314-8060 (on-line version)

deepen cross-level connectivity, albeit at the cost of greater architectural complexity. In maritime contexts where many targets exhibit low resolution or poor contrast such deep necks can inadvertently attenuate crucial object cues as they propagate, yielding diminishing returns for detection precision. YOLOv8 addresses these challenges with a re-balanced neck design and optimized feature-fusion strategies, yet the fundamental tension between multi-scale expressiveness and information preservation remains a focal point for ongoing research.

3.Dataset

The new ship-image corpus was assembled exclusively from publicly available, copyright-free photographs gathered online, yielding an initial pool of approximately 2 100 distinct vessel snapshots captured in real-time maritime settings. Images were selected to span all major visual variations multiple hull viewpoints, scales, background scenes, and common occlusions to ensure broad representativeness across eight principal vessel categories: yacht, patrol boat, submarine, merchant ship, naval vessel, fishing boat, tugboat, and sailboat.

Each frame was meticulously annotated with high-precision bounding boxes and an associated ship-type label, following best practices in automated annotation pipelines for maritime vision (e.g., ACM's recent monocular-camera annotation framework). An additional "mixed" label captures scenes containing overlapping or co-located vessels, boosting the model's ability to generalize to crowded harbour or convoy scenarios.

To alleviate overfitting and enrich sample diversity, classic geometric augmentations random rotations, scaling, and flips were applied, expanding the dataset to over 8 000 training examples. More advanced generative augmentation strategies (e.g. GAN-based DistAug) were also employed to synthetically vary lighting and sea-state conditions. Finally, the expanded corpus was split randomly into 90 % for training and 10 % for held-out testing, following standard deep-learning practice for limited-size datasets

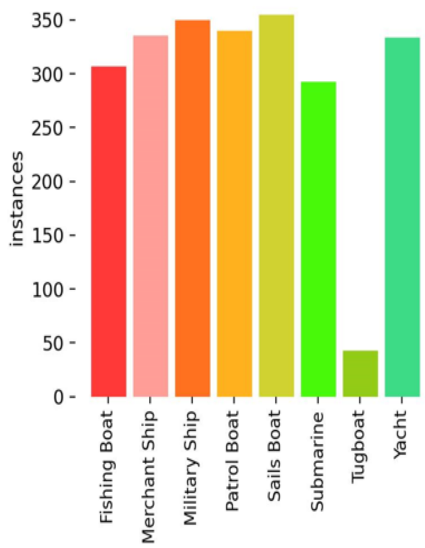

Fig-1 *Different Ship instances based on the classes*

International Journal of Applied Mathematics

Volume 38 No. 12s, 2025

ISSN: 1311-1728 (printed version); ISSN: 1314-8060 (on-line version)

4.Methodology

The dimensions of the anchor boxes denoted by ρ_w and ρ_h must be fixed prior to training, as they directly influence detection quality. To expedite the adjustment of these box sizes, we apply k-means clustering to the set of ground-truth widths and heights. For data of dimensionality d grouped into k clusters and comprising n samples, the runtime complexity is *O(nkd)* Larger *n* thus entails proportionally greater clustering time.

Initialization of Cluster Centre's via Markov chains

Let the true bounding box dimensions be

$$\Phi = \{(w_1, h_1), (w_2, h_2), \ldots, (w_n, h_n)\}$$

1. First centre: randomly select one pair $(w_i, h_i) \in \Phi$ as C_1
2. Proposal distribution for each $\Phi_j \in \Phi$ is computed as

$q(\phi_j) = \frac{d(\phi_j, c_1)}{\sum_{i=1}^{n} d(\phi_i, c_1)} + \frac{1}{n}$ …(eqn.1)

3. Distance metric: replace Euclidean distance by

$d(\phi_j, c_1) = \min\left(1 - \mathrm{IoU}(\phi_j, c_1)\right)$ …(eqn.2)

To obtain remaining *k – 1* seeds, we build *k – 1* Separate Markov chains of length *m*. at each step *t*:

- Draw candidate Φ_t from Φ according to *q(Φ)*
- Compute sampling weight

$p(\phi_t) = \frac{d(\phi_t, C)}{\sum_{i=1}^{n} d(\phi_i, C)}$ …. (eqn.3)

Where C is the set of sensors so far, and $d(\phi_t, C) = \min_{c \in C}\ d(\phi_t, C)$

- Accept Φ_t with probability

$\alpha = \min!\left(1, \frac{p(\phi_t)}{p(\phi_{t-1})} \frac{q(\phi_{t-1})}{q(\phi_t)}\right)$… (eqn. 4)

If α exceeds a uniform random draw u ∼ U (0,1) set the next state to ϕ_t; otherwise repeat ϕ_{t-1}. After m iterations, the chains terminus is used as a new center. Repeat to collect all *k-1* additional canter's, ensuring the distinctness by rejecting any candidate already selected.

Final clustering step With initial centroids C = {c1…,ck}, sample a subset $\Phi_s \subset \Phi$ of size S. Assign each $\phi \in \Phi_S$ to its nearest centroid by the IoU-based distance. Recompute each cluster's center as the mean of its members:

$p_w^{(u)} = \frac{1}{|H|} \sum_{j \in H} w_j\ , \quad p_h^{(u)} = \frac{1}{|H|} \sum_{j \in H} h_j$ … (eqn. 5,6)

International Journal of Applied Mathematics

Volume 38 No. 12s, 2025

ISSN: 1311-1728 (printed version); ISSN: 1314-8060 (on-line version)

where H indexes the points in cluster u. These $(p_w^{(u)}, p_h^{(u)})$ become the final anchor dimensions. By substituting IoU for Euclidean distance and by initializing centers via tailored Markov chains, this scheme yields anchor boxes that closely match the dataset's true aspect-ratio distribution—thereby improving convergence speed and detection reliability.

5.Results and Discussion

A Windows 10 workstation served as the computational platform for both numerical simulations and the transfer-learning pipeline. Processing was carried out on an Intel Core i5-10400F CPU, while all neural-network training and inference tasks ran on an NVIDIA GeForce RTX 2070 Super GPU equipped with 8 GB of GDDR6 memory and 2 560 CUDA cores. All computer-vision experiments utilized the PyTorch deep-learning framework. Input images were uniformly resized to 640 × 640 pixels. Hyperparameters were set as follows: an initial learning rate of 0.01, momentum of 0.10, and weight decay of 0.005. Mini-batches comprised 64 images each.

The selected YOLOv8 variant produced three detection heads operating at distinct spatial scales, enabling the network to localize small, medium, and large ship targets. Anchor initialization was evaluated by testing K=3,6,9,12,15, and 18 cluster centers. Model performance was quantified via the average Intersection over Union (Avg IoU) metric, defined as

$$\text{Avg IoU} = \frac{1}{N}\sum_{j=1}^{N}\left(\max_{k\in\{1,\ldots,K\}} \frac{C_k \cap Y_j}{C_k \cup Y_j}\right) \ldots \text{(eqn 7)}$$

Here, N denotes the total number of ground-truth boxes Y_j, and $\{Ck\}$ are the K anchor proposals. The model's detection accuracy was assessed directly using this Avg IoU score on the held-out test set.

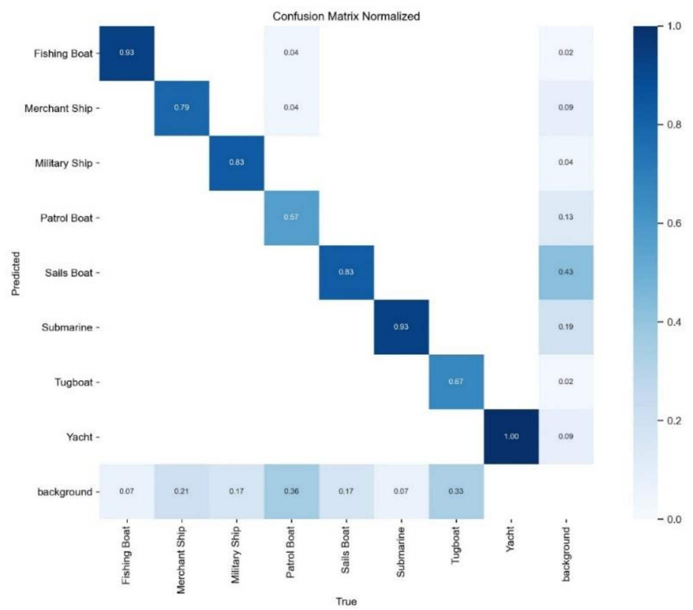

Fig-2: *Confusion matrix showing the accuracy scores of each class trained*

Received: August 01, 2025

International Journal of Applied Mathematics

Volume 38 No. 12s, 2025

ISSN: 1311-1728 (printed version); ISSN: 1314-8060 (on-line version)

The model has F1 scores as 0.83 on the higher side and 0.705 on the lower side. It has performed well on Merchant ships, Fishing boats, Patrol boats and defence vessels and has the lower performance on Yachts, sail boats, submarines and Tugs.

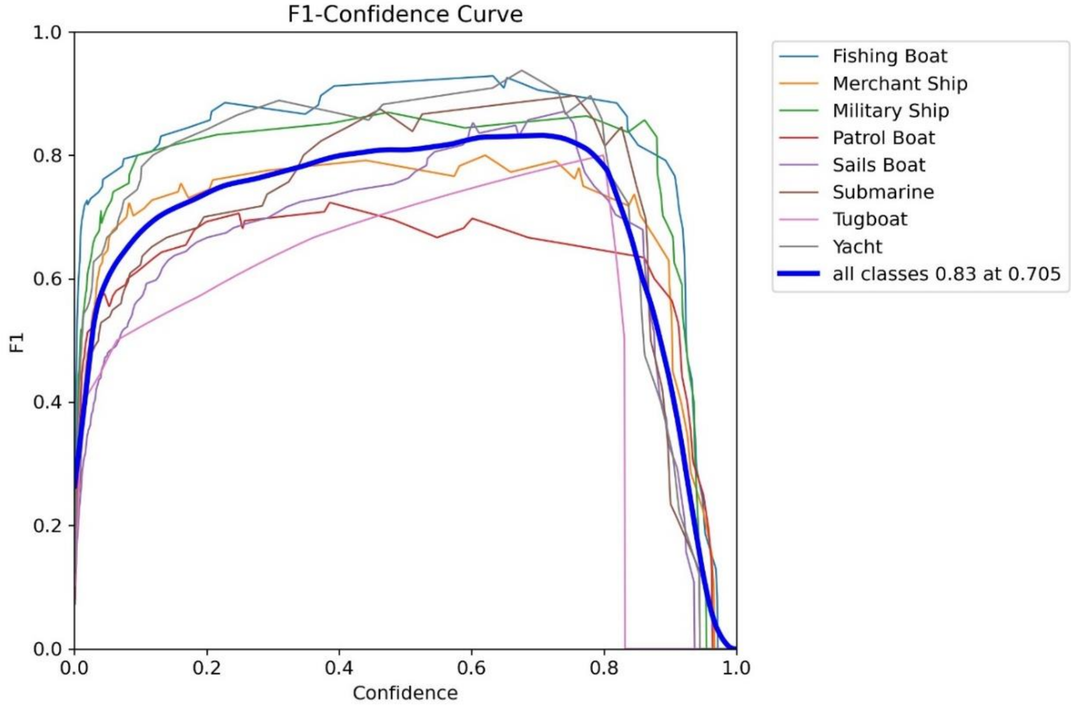

***Fig-3**: F1-Confidence Curve*

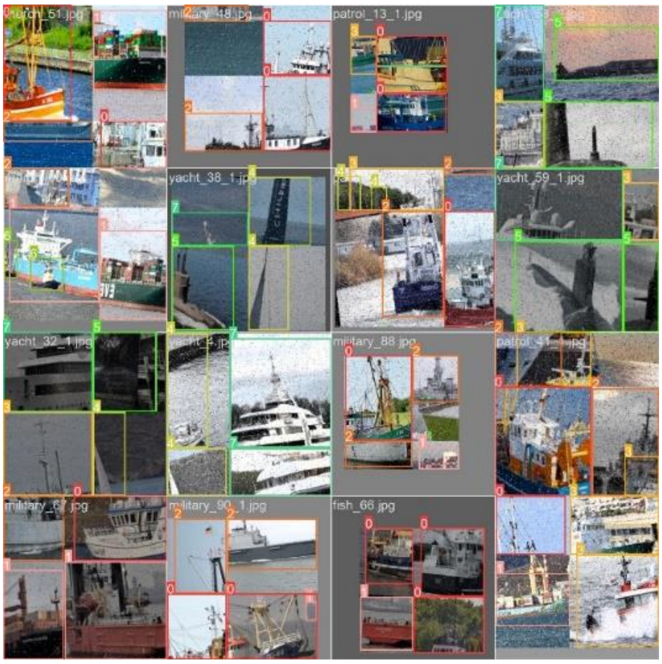

***Fig-4:** Multiclass prediction in the same frame*

Volume 38 No. 12s, 2025

ISSN: 1311-1728 (printed version); ISSN: 1314-8060 (on-line version)

Fig-5: *Test results on Individual classes*

Comparison of the different Yolo models trained on the similar dataset with speed and accuracy

Table-1: *Comparison between different Yolo Models*

FEATURE	YOLOv5	YOLOv7	YOLOv8
Accuracy	0.812	0.819	0.83
Detection Speed per Image (ms)	0.87	0.89	0.80

6.Conclusion:

We showed that it is possible to apply only transfer learning to the YOLOv8m architecture for a narrow task of multi-class detection of maritime vessels. The proposed model surpassed comparative of baselines that were defined by YOLOv5 (81.2%) and YOLOv7 (81.9%) by fine-tuneing pre-trained weights on an augmented 8K-dataset achieving overall classification performance of 83%, respectively. Of importance is that the YOLOv8m model provided better inference accuracy and reduced post-processing latency to 0.80 ms per image. This is a speedup of about 9% compared to previous algorithms, which could be important for deployment on edge devices with limited resources.

Analysis of the performance in the eight categories of vessels uncovered very different strong points in action. The model performed well on the detection of large surface assets such as merchant ships, patrol boats, fishing vessels. By contrast, detection measures decreased in the case of smaller and or more visually complex targets, such as yachts, submarines and tugs there being a relationship between target physical appearance and the reliability of its recognition.

The trade-o between inferring quickly and classifying reliably is found to be well balanced in the above frame work so that the proposed approach is also very promising for real-time applications where latency are extremely important. In particular, the sub-millisecond

Volume 38 No. 12s, 2025

ISSN: 1311-1728 (printed version); ISSN: 1314-8060 (on-line version)

processing time permits integration into autonomous navigations systems for instant collision avoidance and situational awareness. In addition, the models performance to differentiate between questionable types of hulls corresponds with needs for search-and-rescue coordination and regulatory surveillance in, e.g., IMO's Port State Control. Future work will involve adding to the dataset and working towards better recall of smaller vessel classes, with additional focus on incorporating sensor fusion for robust performance in weather conditions.

References

[1] Cheng, Shuxiao, Yishuang Zhu, and Shaohua Wu. Deep learning based efficient ship detection from drone-captured images for maritime surveillance. *Ocean Engineering* **285** (2023): 115440.

[2] Cong-An, Xu, Su Hang, Gao Long, Wu Jun-Feng, Yan Wen-Jun, Jian Tao, and Wang Hai-Yang. Feature aligned ship detection based on improved RPDet in SAR images. *Displays* **74** (2022): 102191.

[3] He, G. *et al.* An improved yolo v4 algorithm-based object detection method for maritime vessels. *Int. J. Sci. Eng. Appl.* **11**, 50–55 (2022).

[4] Humayun, Muhammad Farhan, Farrukh Aziz Bhatti, and Khurram Khurshid. iVision MRSSD: A comprehensive multi-resolution SAR ship detection dataset for state-of-the-art satellite based maritime surveillance applications. *Data in Brief* **50** (2023): 109505.

[5] Jiang, Bitao, Xiaofeng Ma, Yao Lu, Yang Li, Li Feng, and Zhenwei Shi. Ship detection in spaceborne infrared images based on Convolutional Neural Networks and synthetic targets. *Infrared Physics & Technology* **97** (2019): 229-234.

[6] Jiang, P., Ergu, D., Liu, F., Cai, Y. & Ma, B. A review of yolo algorithm developments. *Procedia Comput. Sci.* **199**, 1066–1073 (2022).

[7] Jin, L. & Liu, G. An approach on image processing of deep learning based on improved SSD. *Symmetry* **13**(3), 495 (2021).

[8] Kamalipour, M., Agahi, H., Khishe, M. & Mahmoodzadeh, A. Passive ship detection and classification using hybrid cepstrums and deep compound autoencoders. *Neural Comput. Appl.* **35**(10), 7833–7851 (2023).

[9] Kim, J. H., Kim, N., Park, Y. W. & Won, C. S. Object detection and classification based on YOLO-V5 with improved maritime dataset. *J. Mar. Sci. Eng.* **10**(3), 377 (2022).

[10] Li, H., & Man, Y. Moving ship detection based on visual saliency for video satellite. In *2016 IEEE International Geoscience and Remote Sensing Symposium (IGARSS)*, 1248–1250 (IEEE, 2016).

[11] Li, Y., Fan, Q., Huang, H., Han, Z. & Gu, Q. A modified YOLOv8 detection network for UAV aerial image recognition. *Drones* **7**(5), 304 (2023).

ISSN: 1311-1728 (printed version); ISSN: 1314-8060 (on-line version)

[12] Liu, Shanwei, Weimin Kong, Xingfeng Chen, Mingming Xu, Muhammad Yasir, Limin Zhao, and Jiaguo Li. "Multi-scale ship detection algorithm based on a lightweight neural network for spaceborne SAR images." *Remote Sensing* **14**, no. 5 (2022): 1149.

[13] Lou, Xin, Yicheng Liu, Ziwei Xiong, and Han Wang. Generative knowledge transfer for ship detection in SAR images. *Computers and Electrical Engineering* **101** (2022): 108041.

[14] Lyu, H., Shao, Z., Cheng, T., Yin, Y. & Gao, X. Sea-surface object detection based on electro-optical sensors: A review. *IEEE Intell. Transport. Syst. Mag.* (2022).

[15] Ma, T., Ma, J., & Fu, W. Sea-sky line extraction with linear fitting based on line segment detection. In *2016 9th International Symposium on Computational Intelligence and Design (ISCID)*, Vol. 1, 46–49 (IEEE, 2016).

[16] Matasci, Giona, Jonathan Plante, Kevin Kasa, Payam Mousavi, Andrew Stewart, Andrew Macdonald, Anne Webster, and Jennifer Busler. Deep learning for vessel detection and identification from spaceborne optical imagery. *ISPRS Annals of the Photogrammetry, Remote Sensing and Spatial Information Sciences* **3** (2021): 303-310.

[17] Najibzadeh, M., Mahmoodzadeh, A. & Khishe, M. Active sonar image classification using deep convolutional neural network evolved by robust comprehensive grey wolf optimizer. *Neural Process. Lett.* **55**(7), 8689–8712 (2023).

[18] Nie, S., Jiang, Z., Zhang, H., Cai, B., & Yao, Y. Inshore ship detection based on mask R-CNN. In *IGARSS 2018–2018 IEEE International Geoscience and Remote Sensing Symposium*, 693–696 (IEEE, 2018).

[19] Prasad, D. K., Rajan, D., Rachmawati, L., Rajabally, E. & Quek, C. MuSCoWERT: Multi-scale consistence of weighted edge radon transform for horizon detection in maritime images. *J. Opt. Soc. Am. A* **33**(12), 2491–2500 (2016).

[20] Qi, L. *et al.* Ship target detection algorithm based on improved faster R-CNN. *Electronics* **8**(9), 959 (2019).

[21] Song, H. H., Lee, H. C., Lee, S. J., Jeon, H. S. & Im, T. H. Design of video pre-processing algorithm for high-speed processing of maritime object detection system and deep learning based integrated system. *J. Internet Comput. Serv.* **21**(4), 117–126 (2020).

[22] Song, H., Ren, H., Song, Y., Chang, S. & Zhao, Z. A sea-sky line detection method based on the RANSAC algorithm in the background of infrared sea–land–sky images. *J. Russ. Laser Res.* **42**, 318–327 (2021).

[23] Tian, Y., Khishe, M., Karimi, R., Hashemzadeh, E. & Pakdel Azar, O. Underwater image detection and recognition using radial basis function neural networks and chimp optimization algorithm. *Circuits Syst. Signal Process.* **42**(7), 3963–3982 (2023).

[24] Tian, Z., Shen, C., Chen, H., & He, T. Fcos: Fully convolutional one-stage object detection. In *Proc. of the IEEE/CVF International Conference on Computer Vision*, 9627–9636 (2019).

International Journal of Applied Mathematics

Volume 38 No. 12s, 2025

ISSN: 1311-1728 (printed version); ISSN: 1314-8060 (on-line version)

[25] Wang, B., Su, Y. & Wan, L. A sea-sky line detection method for unmanned surface vehicles based on gradient saliency. *Sensors* **16**(4), 543 (2016).

[26] Wang, G., Wang, X., Fan, B. & Pan, C. Feature extraction by rotation-invariant matrix representation for object detection in aerial image. *IEEE Geosci. Remote Sens. Lett.* **14**(6), 851–855 (2017).

[27] Wu, Y., Chen, Y., Yuan, L., Liu, Z., Wang, L., Li, H., & Fu, Y. Rethinking classification and localization for object detection. In *Proc. of the IEEE/CVF conference on computer vision and pattern recognition*, 10186–10195 (2020).

[28] Xiao, F., Yuan, F. & Cheng, E. Detection and tracking method of maritime moving targets based on geosynchronous orbit satellite optical images. *Electronics* **9**(7), 1092 (2020).

[29] Xin, Z., Kong, S., Wu, Y., Zhan, G. & Yu, J. A hierarchical stabilization control method for a three-axis gimbal based on sea–sky-line detection. *Sensors* **22**(7), 2587 (2022).

[30] Yang, Shizhong, Wei Wang, Sheng Gao, and Zhaopeng Deng. "Strawberry ripeness detection based on YOLOv8 algorithm fused with LW-Swin Transformer." *Computers and Electronics in Agriculture* **215** (2023): 108360.

[31] Yang, T. J., Zhang, S., Zhou, G. Q., & Jiang, C. X. Design of a real-time system of moving ship tracking on-board based on FPGA in remote sensing images. In *International Conference on Intelligent Earth Observing and Applications 2015*, Vol. 9808, 22–27 (SPIE, 2015).

[32] Yang, Z., Li, Y., Wang, B., Ding, S. & Jiang, P. A lightweight sea surface object detection network for unmanned surface vehicles. *J. Mar. Sci. Eng.* **10**(7), 965 (2022).

[33] Yang, Z., Liu, S., Hu, H., Wang, L., & Lin, S. Reppoints: Point set representation for object detection. In *Proc. of the IEEE/CVF International Conference on Computer Vision*, 9657–9666 (2019).

[34] Yasir, Muhammad, Liu Shanwei, Xu Mingming, Sheng Hui, Md Sakaouth Hossain, Arife Tugsan Isiacik Colak, Dawei Wang, Wan Jianhua, and Kinh Bac Dang. Multi-scale ship target detection using SAR images based on improved Yolov5. *Frontiers in Marine Science* **9** (2023): 1086140.

[35] Yutong, G., Khishe, M., Mohammadi, M., Rashidi, S. & Nateri, M. S. Evolving deep convolutional neural networks by extreme learning machine and fuzzy slime mould optimizer for real-time sonar image recognition. *Int. J. Fuzzy Syst.* **24**(3), 1371–1389 (2022).

[36] Zhang, Tianwen, Xiaoling Zhang, Chang Liu, Jun Shi, Shunjun Wei, Israr Ahmad, Xu Zhan et al. Balance learning for ship detection from synthetic aperture radar remote sensing imagery. *ISPRS Journal of Photogrammetry and Remote Sensing* **182** (2021): 190-207.

Received: August 01, 2025

ISSN: 1311-1728 (printed version); ISSN: 1314-8060 (on-line version)

[37] Zhao, H., Zhang, H., & Zhao, Y. Yolov7-sea: Object detection of maritime uav images based on improved yolov7. In *Proc. of the IEEE/CVF Winter Conference on Applications of Computer Vision*, 233–238 (2023).

[38] Zheng, Y., & Zhang, S. Mcships: A large-scale ship dataset for detection and fine-grained categorization in the wild. In *2020 IEEE International Conference on Multimedia and Expo (ICME)*, 1–6 (IEEE, 2020).